Original Article

Hypoxia induces tumor cell growth and angiogenesis in non-small cell lung carcinoma via the Akt-PDK1-HIF1α-YKL-40 pathway

Yushan Miao[1#], Wei Wang[1#], Yaping Dong[2#], Jiaxun Hu[1], Kunchen Wei[1], Shuo Yang[1], Xueli Lai[3], Hao Tang[1]

[1]Department of Respiratory and Critical Care Medicine, Changzheng Hospital, Second Military Medical University, Shanghai 200003, China; [2]The Graduate School of Fujian Medical University, Fuzhou 350122, China; [3]Department of Nephrology, Shanghai Changhai Hospital, Second Military Medical University, Shanghai 200433, China

Contributions: (I) Conception and design: H Tang, X Lai, Y Miao, W Wang; (II) Administrative support: X Lai, H Tang; (III) Provision of study materials or patients: J Hu, K Wei, S Yang; (IV) Collection and assembly of data: Y Miao, W Wang, Y Dong; (V) Data analysis and interpretation: Y Dong, S Yang, J Hu; (VI) Manuscript writing: All authors; (VII) Final approval of manuscript: All authors.

[#]These authors contributed equally to this work.

Correspondence to: Xueli Lai, MD. Department of Nephrology, Shanghai Changhai Hospital, Second Military Medical University, 168 Changhai Road, Shanghai 200433, China. Email: laixueli_changhai@163.com; Hao Tang, MD, PhD. Department of Respiratory and Critical Care Medicine, Changzheng Hospital, Second Military Medical University, 415 Fengyang Road, Shanghai 200003, China. Email: tanghao_0921@126.com.

Background: As one of the most common forms of cancer, non-small cell lung carcinoma (NSCLC), is characterized by oxygen deprivation (hypoxia). The transcription factor hypoxia-inducible factor (HIF)-1α is a major mediator which responds hypoxia and regulates many contributing factors. The various modes of hypoxia regulation are frequently the focus of research studies. With reference to previous published research, we hypothesized that hypoxia promotes the growth and angiogenesis of NSCLC via the Akt-PDK1-HIF1α-YKL-40 pathway, and verified it.

Methods: We mainly investigated changes in related factor expression between differently treated CL1-5 cells. We carried out overexpression and underexpression transfection, Western blot, rt-PCR and ELISA, and observed cellular biological behaviors by CCK-8 migration and invasion assay, and tube formation assay.

Results: A hypoxic environment significantly increased the phosphorylation of Akt and PDK1 in mitochondria. The hypoxia-induced accumulation of p-Akt in mitochondria activated PDK1 phosphorylation, promoted the expression of HIF1α, and the expression of YKL-40. The overexpression of YKL-40 promoted the proliferation, migration, invasion and tubule formation of CL1-5 cells.

Conclusion: A hypoxic tumor microenvironment can promote the expansion and angiogenesis of NSCLC cells through the Akt-PDK1-HIF1α-YKL-40 pathway. This may provide a new mechanism and potential interventional target for anti-vascular lung cancer therapy.

Keywords: Hypoxia; Akt; hypoxia-inducible factor-1α (HIF-1α); YKL-40; non-small cell lung carcinoma (NSCLC)

Submitted Dec 18, 2019. Accepted for publication Mar 10, 2020.
doi: 10.21037/tcr.2020.03.80
View this article at: http://dx.doi.org/10.21037/tcr.2020.03.80

Introduction

Lung cancer is the most common form of cancer and the leading cause of cancer-related deaths (1). Non-small cell lung carcinoma (NSCLC), which accounts for 85% of lung cancer cases, manifests in the form of tumorous growths. During the progressive stage of this solid tuberous tumor, a disordered, inefficient neovascular system and over-rapid growth of tumor cells result in intratumoral oxygen deprivation. This unruly hypoxic microenvironment in turn promotes tumor malignity (2). Many studies have shown

that a hypoxic microenvironment can induce instability in the gene phenotype of tumor cells as well as tumor angiogenesis, therefore promoting tumor metastasis (3-6). HIF, a transcription factor, plays a critical role in malignant tumor adjustment in a hypoxic microenvironment (7,8), with VEGF (vascular endothelial growth factor) and erythropoietin as two of its common target genes. It has been reported that HIF1α can regulate tumor angiogenesis by inducing the secretion of VEGF (6), which is one of the most predominant angiogenic factors in human lung cancer (6).

A recent study (9) focusing on glioma showed a new Akt-PDK1 signal in which hypoxic tumors recruited a pool of active Akt to mitochondria, culminating with the phosphorylation of pyruvate dehydrogenase kinase 1 (PDK1). In cases of severe hypoxia, phosphorylation acts to strengthen the tumor and preserve tumor cell proliferation. Another study (10) showed that inhibition of PDK in mitochondria suppressed HIF1a signaling and angiogenesis in cancer. PDK inhibited the ubiquitin degradation of HIF1α through PHD-pVHL dysfunction, which was a result of a decrease of PDH and its downstream production of 2-oxoglutarate in the Krebs cycle (10-15) and an upregulated level of HIF1α. To date, research into NSCLC has failed to establish whether the mitochondrial Akt-PDK1 signaling pathway is induced by hypoxia or if it plays a role in promoting tumor angiogenesis through HIF1α expression.

Concerning the mechanisms of HIF1α in angiogenesis, excluding VEGF, HIF1α has been found to activate the TGF-β/smad3 pathway and prompt fibrosis in renal tubular epithelial cells (16). TGF-β stimulates vascular smooth muscle cell proliferation (17,18) and inhibits apoptosis (19) through the Smad3-related pathway. YKL-40 is observed to be upregulated by the TGF-β signaling pathway (20,21) and plays an important role in the regulation of epithelial-mesenchymal transition (EMT) and tumor invasion (22). YKL-40 upregulates the expression of VEGF and promotes endothelial cell angiogenesis (23-26). It is widely reported that there is correlation between the serum level of YKL-40 and poor prognosis in various cancers (27,28) and it acts as an angiogenic factor in the promotion of tumor angiogenesis (25,29). However, the role of YKL-40 in angiogenesis of lung cancer and its association with hypoxia has not yet been sufficiently explored.

To observe the possible hypoxia-response mechanisms in NSCLC cells, we hypothesized that the activation of the AKT-PDK1 signaling pathway in mitochondria results in the upregulation of HIF1α and, consequently, tumor angiogenesis and invasiveness in NSCLC cells is promoted through an increase in the secretion of TGF-β/YKL-40/VEGF. We studied human lung adenocarcinoma cell lines CL1-5 both *in vitro* and *in vivo* and particularly examined the function of YKL-40 in this possible hypoxia-induced pathway.

Methods

Materials and reagents

Abs against phospho-Akt1, Akt1, phospho-Akt2, PDK1, phospho- PDK1, Smad3, phospho-Smad3, and β-actin were ordered from Cell Signaling Technology (CST). Abs against cox4, Akt2, β-tubulin were purchased from Proteintech (WUHAN SANYING). Abs against YKL-40 and HIF1α came from Abcam. HIF-1α antibody was ordered from NOVUS.

Cell culture

A CL1-5 lung adenocarcinoma cell line was established by selecting increasingly invasive cancer cell populations from a clonal cell line of human lung adenocarcinoma CL1. CL1-5 is a subline that was selected from the parent cell line CL1-0 cells cultured on a polycarbonate membrane coated with Matrigel in a Transwell invasion chamber. For a controlled experiment, CL1-5 cells were always cultured in two different groups. CL1-5 cells in the normoxic treatment group were cultured in 37 ℃, 21%O_2 and 5%CO_2 incubators. The cells in the hypoxic group were cultured in 37 ℃, 1%O_2, 5%CO_2 and 94%N_2 incubators. The cells were cultured in groups for 0, 24, 48, and 96 h in the first HIF1α experiment, with the most obvious difference in mass shown in the 24-h group; therefore, all of the cells in the following experiments were cultured for 24 h.

Western blot assay

Protein Akt/PDK1 was extracted using mitochondrial protein extraction kits (Biobox). Whole cell extracts were homogenized in RIPA lysis buffer and centrifuged at 12,000 g for 15 min. Protein concentrations were measured using the bicinchoninic acid assay. Immunoblotting was performed using specific primary antibodies, and immunocomplexes were incubated with fluorescein-conjugated secondary antibody, then detected using an Odyssey fluorescence scanner (Li-Cor, Lincoln, NE, USA).

Enzyme-linked immunosorbent assay

We collected the supernatants of the groups of differently cultured cells. TGF-β, YKL-40 and VEGF levels were quantified in duplicate using ELISA kits in every experiment, in accordance with the manufacturer's instructions.

Akt siRNA transfection

According to the Akt1/2 sequence information in Genebank, 6 interference sequences, Akt1-siRNA1, Akt1-siRNA2, Akt1-siRNA3, Akt2-siRNA1, Akt2-siRNA2, Akt2-siRNA3 and control-siRNA were constructed. They were inserted into plasmid containing the reporter gene cGFP marker and Neomycin resistance gene for the construction of the siRNA recombinant plasmid. The recombinant plasmid was then transformed into a competent Escherichia coli strain DH5α cell. Several single colonies were selected in the culturing process of a small number of bacteria. After the recombinant plasmid had been successfully constructed, the plasmid was then extracted and transfected into CL1-5 cells once the cell coverage rate had reached 70%. After transfection for 48 h, the mRNA expressions of Akt1 and Akt2 were detected by qRT-PCR to determine the effect of siRNA. We selected those which had the best silencing effect on siRNA for subsequent experiments, which were named control siRNA, Akt1 siRNA, and Akt2 siRNA, respectively (*Figure S1*).

Akt shRNA stably transfected strain establishment

Akt1/2 shRNA was synthesized according to the selected Akt1/2 siRNA, as described above. Short hairpin RNA (shRNA) sequences were constructed into LV3 vectors and then tested for inhibitory activity via transient transfection into 293T cells. The templates of shRNA for Akt2 and control shRNA were designed with the loop structure TTCAAGAGA. The most effective sequence specifically for Akt shRNA appeared to be Akt2 shRNA (*Figure S2A*), which were inserted along with control scramble shRNA into the BamHI/EcoRI restriction sites of LV, to make complete vectors, named Akt2-shRNA and scramble-shRNA. After transfection to 293T cells, packed lentiviruses were harvested and then stably transfected to CL1-5 cells in the presence of 5 μg/mL polybrene. After 2–3 weeks, single independent clones were randomly isolated and plated separately to be tested for Akt2 RNA. In this way, two CL1-5 lines were established: one expressing an AKT2-specific shRNA, leading to stable underexpression of AKT2; and the other, scramble shRNA, as a negative control.

Real-time PCR analysis

Total RNA was isolated using Trizol reagent (Aidlab), and 2 mg total RNA was reverse-transcribed using Reverse Transcription Reagents (TINGEN). Quantitative PCR was performed using SYBR Green PCR Master Mix (VAZYME). The mRNA levels of specific genes were normalized to that of actin. The mRNA levels of the indicated genes were analyzed using SYBR Green PCR Master Mix (VAZYME). The primer sequences used can be found in *Table 1*. Thermal cycling conditions consisted of an initial denaturing step (95 ℃, 2 min) followed by 40 cycles of denaturing (95 ℃, 15 s), annealing (60 ℃, 15 s), and extending (72 ℃, 45 s). The specificity of the product made was controlled via a melting curve.

Cell viability assay

Cell viability was determined by colorimetric assay with Cell Counting Kit-8 (CCK-8; BD Biosciences). Briefly, cells were plated at 4×10^3 cells per well in triplicate in 96-well plates to measure cell viability, 10 μL of CCK-8 reagents were added to each well and then incubated at 37 ℃ for 1 h. Subsequently, the absorbance rate in each well was read with a spectrophotometric plate reader at 450 nm. The results were expressed as the percentage of viable cells over cells in the control group.

Cell migration and invasion assay

The migration and invasion potential were determined on gelatin-coated Transwell inserts with 8 μm pore size (BD Biosciences). For this, cells were trypsinized and resuspended in 0.1% FCS containing medium. One hundred and fifty μL of a cell suspension containing 5×10^4 cells were added to the Transwell in triplicate per condition. 10% FCS or 0.1% FCS was added to the lower wells as chemoattractants. Cells that had migrated/invaded and appeared on the bottom surface of the Transwell insert membrane were fixed with 75% methanol/25% acidic acid for 20 min and stained with 0.25% Coomassie blue in 45% methanol/10% acetic acid, followed by washing with demi water. The membranes were subsequently cut out and mounted on microscopic slides for quantification.

Table 1 Sequence of primers for real-time PCR

Primer	Sequence (5' to 3')
Akt1 forward primer	TATTGTGAAGGAGGGTTG
Akt1 reverse primer	ATTCTTGAGGAGGAAGTAG
Akt2 forward primer	ACTGAGGAGATGGAAGTG
Akt2 reverse primer	CCAAGGAGTTTGAGATAGTC
PDK1 forward primer	CCTAGAGGGTTACGGGACAG
PDK1 reverse primer	CGTCGTCATGTCTTTGGGTT
HIF1α forward primer	ATGTAATGCTCCCCTCACCC
HIF1α reverse primer	CCTGAATCTGGGGCATGGTA
YKL-40 forward primer	CGCAAATGGGCGGTAGGCGTG
YKL-40 reverse primer	CTTCCTAGAGCATGGCTACGTA
GAPDH forward primer	TCAAGAAGGTGGTGAAGCAGG
GAPDH reverse primer	TCAAAGGTGGAGGAGTGGGT
Actin forward primer	CATGTACGTTGCTATCCAGGC
Actin reverse primer	CTCCTTAATGTCACGCACGAT

Representative pictures of the membranes with cells were acquired at 5× magnification and the total number of cells on 50 individual fields per membrane was counted; average numbers and standard deviation of invading cells for every condition were calculated.

Tube formation assay

The angiogenic activity was assessed using an *in-vitro* angiogenesis assay kit according to the manufacturer's instructions (Cayman Chemical, USA). Martigel was pre-placed in 96-well plates, and 1×10^4 HMVECs (human microvascular endothelial cells) were added to matrigel and cultured. The cells in each group were treated with conditioned medium for 24 h, and the number of tubules was observed. All experiments were conducted independently and each was carried out at least three times.

Construction of PDK-1/HIF1α/YKL-40 overexpression vectors

According to the NCBI human PDK-1/HIF1α/YKL-40 sequences, PDK-1/HIF1α/YKL-40 genes were synthesized. They were inserted into plasmid containing the reporter gene cGFP marker and Neomycin resistance gene for construction of recombinant plasmids. The recombinant plasmids were then transformed into competent Escherichia coli strain DH5α cells. Several single colonies were selected in the culturing process of a small number of bacteria. After the recombinant plasmids had been successfully constructed, the plasmids were extracted and transfected into CL1-5 cells once the cell coverage rate had reached 70%. After transfection for 48 h, the mRNA expressions of PDK-1, HIF1α, and YKL-40 were detected by qRT-PCR to determine the levels of overexpression.

Tumor xenografts

For tumor growth, 2×10^6 cells in 200 μL PBS were administered by subcutaneous injection into the right flank of 6-to-8-week-old immunocompromised male mice (NSG, NOD.Cg-*Prkdc*^{scid} *Il2rg*^{tm1Wjl}*/SzJ*). Each group consisted of eight mice. Tumor growth was monitored every 4 days, and the mice were sacrificed on day 32. Tumor volume was calculated with slide calipers using the following formula: V = width × width × length × 0.5, wherein V is volume (mm^3).

Immunohistochemical test

Tumor tissues were divided and fixed in phosphate-buffered neutral formalin, embedded in paraffin, and cut into 5-μm-thick sections. The sections were incubated with primary

rabbit anti-Ki67/vWF antibody (Abcam) at 4 ℃ overnight and then with horseradish peroxidase–conjugated secondary antibody at 37 ℃ for 30 min. Vector ABC kit (Vector Laboratories, Burlingame, CA, USA) and DAB reagent (Dako, Glostrup, Denmark) were employed in the detection procedure. All slides were analyzed and photographed with an Olympus microscope (Olympus, Tokyo, Japan).

Statistical analysis

Differences among variables were assessed by Student's *t*-test. Data are presented as the mean± standard error of the mean (SEM) unless otherwise indicated. Difference were considered statistically significant when $P<0.05$. Statistical analyses were performed with SPSS 16.0 software (SPSS, Chicago, IL, USA).

Results

Hypoxia induces the recruitment of Akt and PDK1 in mitochondria and HIF1α accumulation

To explore the differences in protein expression caused by hypoxia exposure, CL1-5 cells were cultured in normoxic (21% O_2) and hypoxic (1% O_2) environments for 0, 24, 48 and 96 h. Western blot analysis showed that the expression of HIF1α was higher after hypoxic culturing compared with the normoxic one, particularly for a period of 24 h (*Figure 1A*). Each group of cells was subsequently cultured for 24 h. Hypoxic culture significantly increased the phosphorylation levels of Akt1, Akt2 and PDK1 in mitochondria (*Figure 1B*). Expressions of HIF1α and YKL-40 and the phosphorylation of Smad3 were upregulated under hypoxia (*Figure 1C*). Hypoxic treatment also increased the secretion of TGF-β, YKL-40, and VEGF (*Figure 1D*). Thus, hypoxia induced the phosphorylation of Akt1, Akt2, and PDK1 in mitochondria and Smad3, as well as the expression of HIF1α, YKL-40, TGF-β, and VEGF. Preliminarily, it could be observed that the hypoxic culture activated the Akt-PDK1 signal pathway, as well as cell factors HIF1α/TGF-β/p-Ssmad3/YKL-40/VEGF. We then examined the accurate interaction between the factors.

The accumulation of Akt-PDK1 promoted HIF1α expression, which induced malignant phenotype of CL1-5 cells under hypoxia

In the next stage of our study, we chose the most effective Akt1 siRNAs and Akt2 siRNAs from all of the siRNAs that we designed and synthetized (*Figure S1*). CL1-5 cells were first transfected with control siRNA or Akt1 siRNA or Akt2 siRNA for 48 h and then cultured normoxicly or hypoxicly for another 24 h. Akt1/Akt2 siRNA inhibited the hypoxia-induced phosphorylation of Akt1/Akt2 and PDK1 in mitochondria (*Figure 2A*). Cells transfected by PDK1 OE (*Figure S2B*) had significant HIF1α expression, which was furthered by hypoxia treatment (*Figure 2B*). Under hypoxia, PDK1 OE transfection had little effect on the production of Akt/p-Akt in CL1-5 cells (*Figure 2C*). CL1-5 cells transfected with PDK1 OE, LV-Akt2 shRNA (*Figure S2A*) showed lower expression of Akt and p-Akt, compared with LV-scramble shRNA-infected CL1-5 cells (*Figure 2C*), indicating that PDK1 had no influence on Akt or its phosphorylation. Thus, this supports the idea that hypoxia-induced Akt2 phosphorylation leads to PDK1 phosphorylation, sequentially boosting the expression of HIF1α in CL1-5 cells. The phosphorylation of Smad3 and hypoxia-induced secretion of TGF-β was blocked by Akt siRNA, as was the increase in the production of HIF1α/YKL-40/VEGF (*Figure 2D*,*E*). The downstream pathway TGF-β/smad3 and factors YKL-40 and VEGF are associated with the Akt-PDK1-HIF1α pathway.

At a cellular level, the growth, migration, invasion, and tube formation activities of CL1-5 cells, which are promoted in hypoxic environment, were restricted when the cells had been transfected with Akt siRNA (*Figure 3A*,*B*,*C*,*D*). The upregulation of phosphorylation of Akt in hypoxia-cultured CL1-5 cells upregulated the phosphorylation of PDK1, induced the high level of HIF1α, and eventually prompted tumor angiogenesis and malignance.

HIF1α is responsible for expression and secretion of YKL-40 in CL1-5 cells

We next constructed HIF1α overexpression vector according to NCBI human HIF1α gene order and YKL-40 overexpression vector, and validated its stabilization and large quantity of expression through qRT-PCR (*Figure S3A*,*B*). HIF1α OE transfected CL1-5 cells clearly created more YKL-40 and phosphorylated Smad3 under hypoxia, although there was no difference in Akt1/Akt2 or phosphorylation proteins, whether they had been transfected or not (*Figure 4A*). HIF1α OE treatment regained p-Smad3 and YKL-40, which were reduced by Akt2 shRNA (*Figure 4B*). However, YKL-40 OE did not change Akt2 shRNA-induced phosphorylation of Smad3

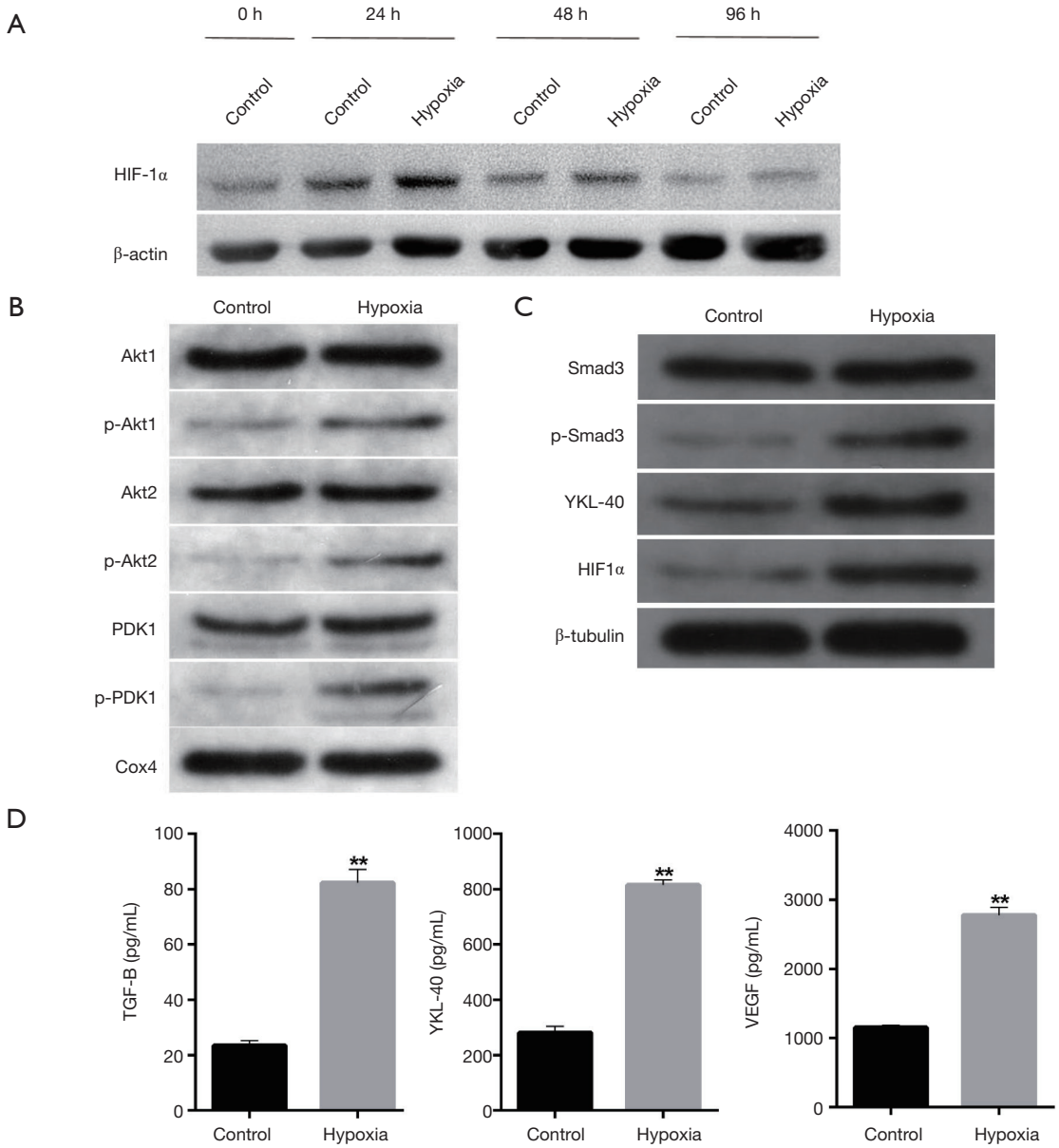

Figure 1 Changes in protein expression in CL1-5 cells under hypoxia. (A) Western blots showing the expression of HIF1α changed over time under hypoxic or normoxic exposure. B-actin set as internal reference. (B) Representative Western blots pictures; total Akt1, Akt2, and PDK1 showed little difference in a hypoxic or normoxic environment. Cox4 set as internal reference of mitochondrial proteins. (C) A representative Western blot picture of cytoplasm proteins setting β-tubulin as reference. (D) ELISA's data of mass of TGF-β, YKL-40, and VEGF are depicted as the mean of three independent experiments measured in triplicate ± SEM (**, P<0.01).

(*Figure 4C*). Hypoxic culture promoted the secretion of TGF-β/YKL-40/VEGF, and HIF1α OE further promoted the secretion of these factors in CL1-5 cells (*Figure 4D*). HIF1α OE transfection elevated the level of TGF- β/YKL-40/VEGF in Akt2 shRNA-infected CL1-5 cells (*Figure 4E*). The results above indicate that HIF1α promotes YKL-40 expression and secretion through TGF- β/smad3 signal in CL1-5 cells.

YKL40 is a key mediator of the Akt-PDK1-HIF1α signaling pathway

To explore the association between YKL-40 secretion

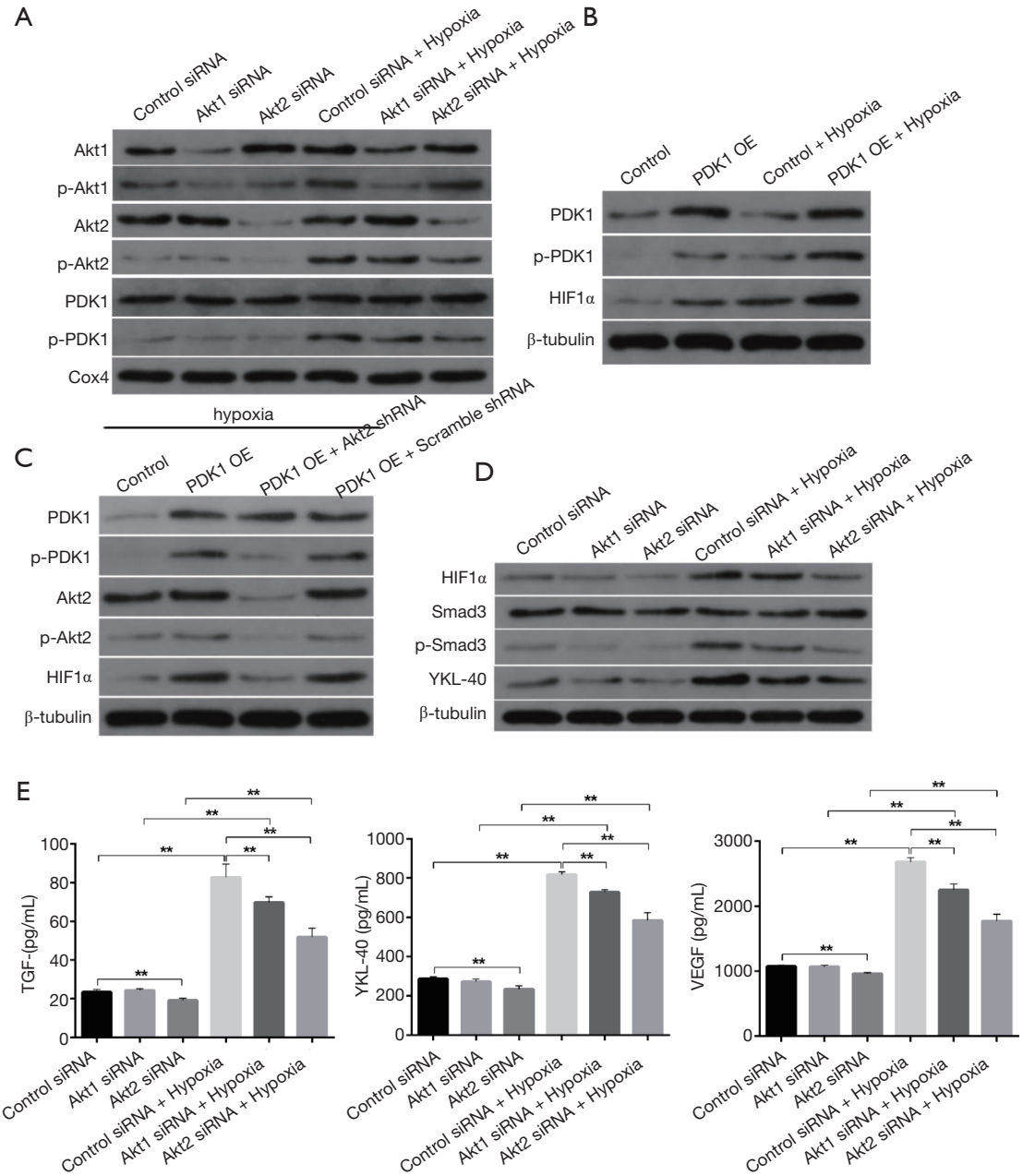

Figure 2 The accumulation of Akt-PDK1 promoted HIF1α expression. (A) The Western blot test of mitochondrial proteins showing that the levels of Akt1, Akt2, and PDK1 phosphorylation increased in a hypoxic environment, and Akt1 siRNA inhibited the expression of Akt1 and its phosphorylation and PDK1 phosphorylation, as did Akt2. Cox4 set as internal reference of mitochondrial proteins. (B) Band map of CL1-5 cells protein expression in each group; control, transfected by blank vector + normoxic culture; PDK1 OE, transfected by PDK1 overexpression vector + normoxic culture; control + hypoxia, transfected by blank vector overexpress + hypoxia culture; PDK1 OE + hypoxia, transfected by PDK1 overexpression vector + hypoxia culture. (C) Band map of cell protein expression under hypoxia; control, CL1-5 cells+ transfected by blank vector; PDK1 OE, CL1-5 cells + transfected by PDK1 ion vector. **, P<0.01. (D) B-actin set as cytoplasmic internal reference. The levels of HIF1α, YKL-40, and p-Smad3 markedly increased under hypoxia, and Akt1/Akt2 siRNAs inhibited the expression of downstream proteins PDK1, HIF1α, YKL-40, and p-Smad3. (E) ELISA assays of TGF-β/YKL-40/VEGF mass in liquid supernatant. The secretion of TGF-β/YKL-40/VEGF was promoted by hypoxia and restricted by Akt2 siRNA (results of Akt1 are not statistically significant). Data are depicted as mean of three independent experiments measured in triplicate ± SEM (**, P<0.01).

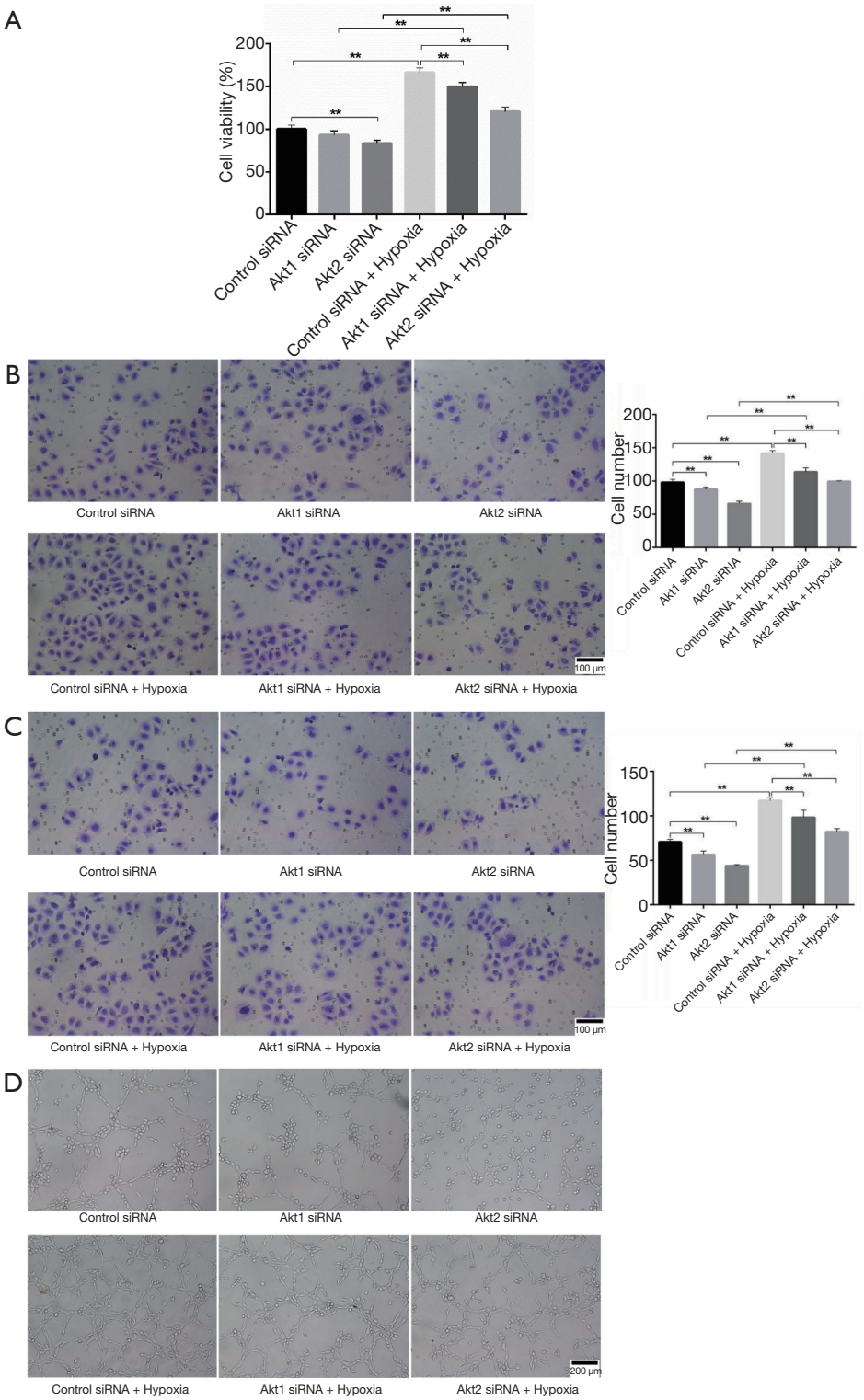

Figure 3 The accumulation of Akt-PDK1 induced malignant phenotype of CL1-5 cells under hypoxia. (A) CCK-8 assay result shows viability of CL1-5 cells. Representative images of (B) migration, (C) invasion, (D) tube-formation assays showing the positive effects of hypoxia and the negative effects of Akt1/Akt2 siRNA. Scale bars =100 μm (B,C), 200μm (D) Quantitative results for migration (B), invasion (C) data have been shown. Dates are depicted as the mean of three independent experiments measured in triplicate ± SEM (**, P<0.01).

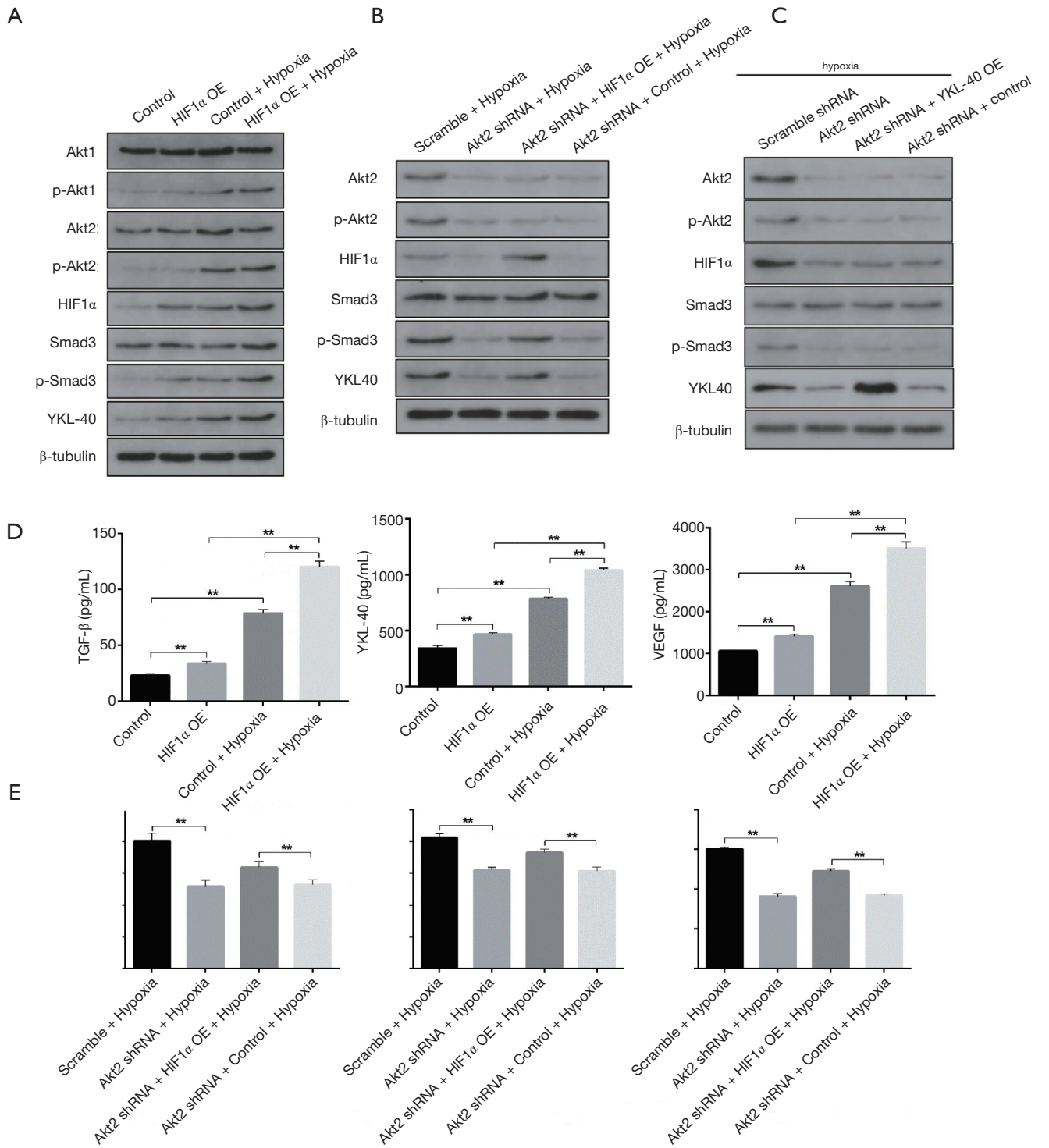

Figure 4 HIF1α is responsible for expression and secretion of YKL-40 in CL1-5 cells. (A) Band map of CL1-5 cells protein expression in each group; control, transfected by blank vector + normoxic culture; HIF1α OE, transfected by HIF1α overexpression vector + normoxic culture; control + hypoxia, transfected by blank vector + hypoxia culture; HIF1α OE + hypoxia, transfected by HIF1α overexpression vector + hypoxia culture. (B) Band map of cell protein expression. (C) Band map of CL1-5 cells protein expression under hypoxia in each group. (D) ELISA assays of TGF-β/YKL-40/VEGF mass in liquid supernatant of each group. (E) ELISA assays of TGF-β/YKL-40/VEGF mass in liquid supernatant of each group. **, P<0.01.

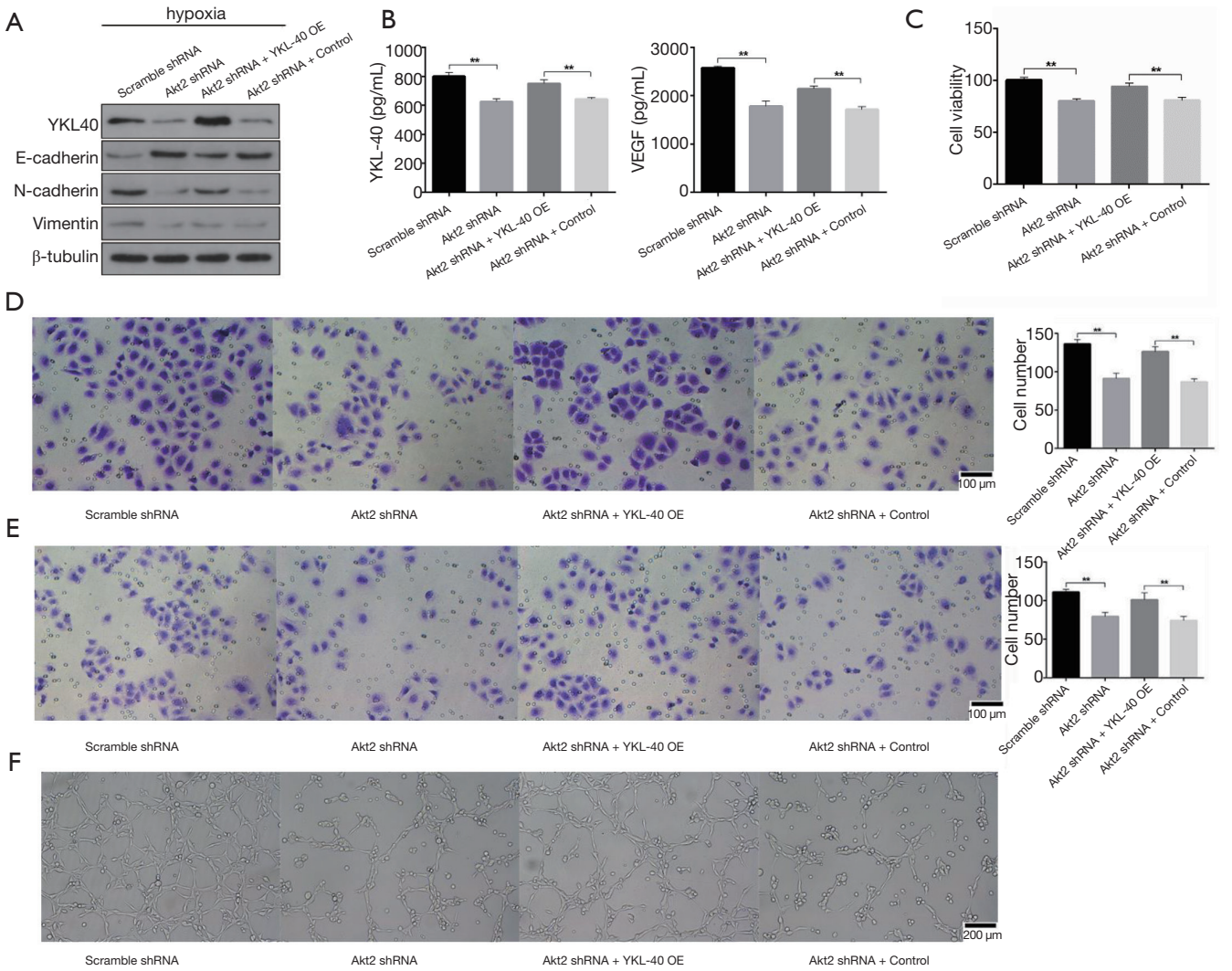

Figure 5 YKL40 is a key mediator of the Akt-PDK1-HIF1α signaling pathway. (A) Western blot band map of CL1-5 cells proteins expression under hypoxia in each group. (B) ELISA assays of YKL-40 and VEGF mass in liquid supernatant of each group. (C) CCK-8 kit assay result shows viability of CL1-5 cells. Representative images of (D) migration, (E) invasion, (F) tube-formation assays. Scale bars =100 μm (D,E), 200 μm (F) Quantitative results for migration (D), invasion (E) data have been shown. Dates are depicted as the mean of three independent experiments measured in triplicate ± SEM (**, P<0.01).

and cell function, we found that Akt2 shRNA stable transformants reduced the production of YKL-40, N-cadherin and Vimentin but increased E-cadherin. YKL-40 OE had N-cadherin and Vimentin regained and E-cadherin reduced (*Figure 5A*). The secretion levels of YKL-40 and VEGF wer low in Akt2 shRNA infected CL1-5 cells, and YKL-40 OE transfection elevated the level (*Figure 5B*). The loss of epithelial surface marker E-cadherin, and the acquisition of mesenchymal markers including Vimentin and N-cadherin are the hallmarks of EMT in the invasion and progress of malignant tumors (30). The proliferation, migration, invasion, and tube-formation of tumor cells were then studied. Akt2 shRNA inhibited cell growth abilities under hypoxia and YKL-40 OE promoted these abilities. The expression of YKL-40 accelerated tumor cells' proliferation, migration and invasion, and provoked endothelial cell tube formation (*Figure 5C,D,E,F*). These suggest that YKL-40, upregulated under hypoxia by the Akt-PDK1-HIF1α-TGFβ/Smad3 signaling pathway, promoted tumor deterioration through

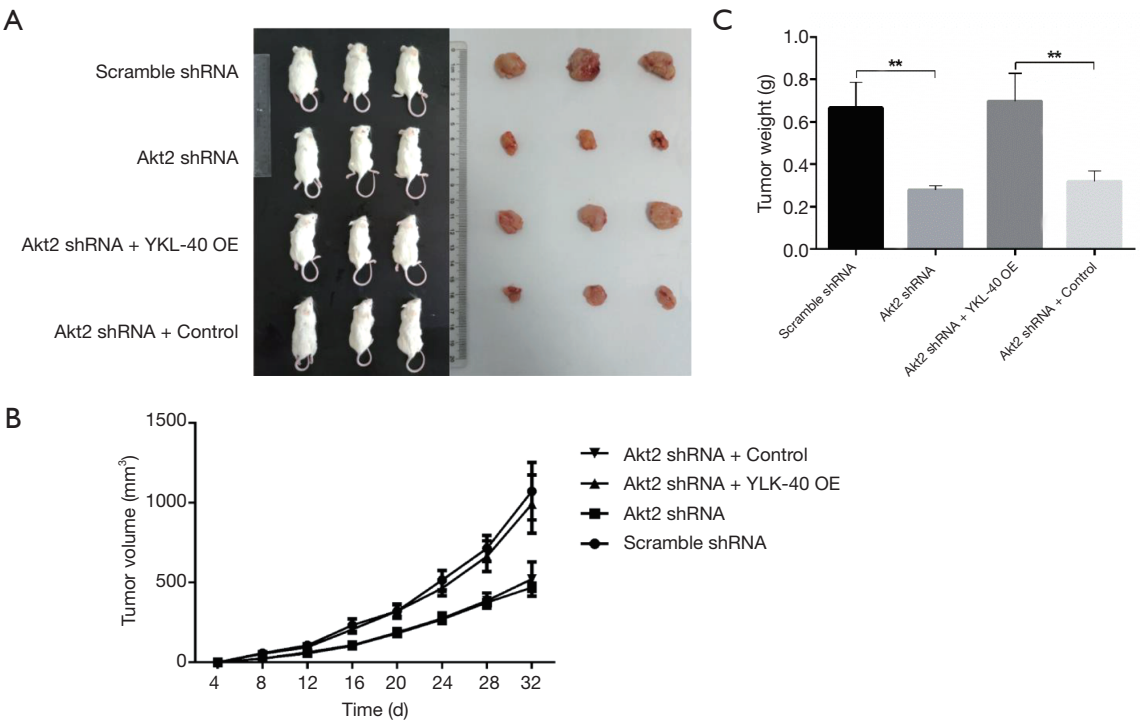

Figure 6 Growth of xenograft of NSCLC could be targeted by Akt inhibition but rescued by YKL-40 expression. (A) Tumor volume on day 32 after subcutaneous transplant of cells in mice; (B) tumor volume increased with time; one-way analysis of variance analysis is used in data statistics, and the error line denotes SD; (C) tumor weight on day 32 in mice after tumor cell transplant. **, P<0.01.

EMT and angiogenesis in non-small cell lung cancer.

Growth of xenograft of NSCLC could be targeted by Akt inhibition but rescued by YKL-40 expression

To confirm the regulating effects of Akt and YKL-40 in vivo, we injected Akt2 shRNA and/or YKL-40 OE-treated CL1-5 cells into mice subcutaneously. At 32 days after transplant, tumor volume increased slower in the mice injected with Akt2 shRNA than in the scramble mice. While the tumor volumes of the YKL-40 OE-infected mice were larger (*Figure 6A,B*), the tumor weight measured on day 32 showed similar statistics as tumor volume (*Figure 6C*). This showed that the growth of xenograft of NSCLC could be targeted by Akt inhibition but rescued by YKL-40 expression.

YKL-40-induced angiogenesis and tumor proliferation in vivo

To further explore the role YKL-40 plays in the mouse model above, we tested the relevant factors in xenograft. Proteins inside tumor cells showed corresponding changes. Compared with scramble shRNA-transfected mice, the tumors of the mice with Akt2 shRNA had a lower level of phosphorylation of PDK1 and Smad3, lower expression of HIF1α, TGF-β, YKL-40, N-cadherin, vimentin and VEGF, and a higher level of E-cadherin expression. YKL-40 OE infection resulted in the upregulation of TGF-β, YKL-40, N-cadherin, vimentin and VEGF, and downregulation of E-cadherin, but did not affect Akt2/p-Akt2, PDK1/p-PDK1, HIF1α, or Smad3/p-Smad3 (*Figure 7A*). Immunohistochemical staining showed that the positive expression rates of Ki67 and vWF in tumor cells of Akt2 shRNA mice was significantly decreased, indicating the inhibition of cell proliferation and angiogenesis. YKL-40 OE raised Ki67 and vWF positive rates (*Figure 7B,C*). This proved that the production and secretion of YKL-40, which was activated by the Akt-PDK1-HIF1α signaling pathway, promoted tumor proliferation and angiogenesis with the assistance of VEGF in our mouse model.

Discussion

In this study, we found a new regulation pathway in the

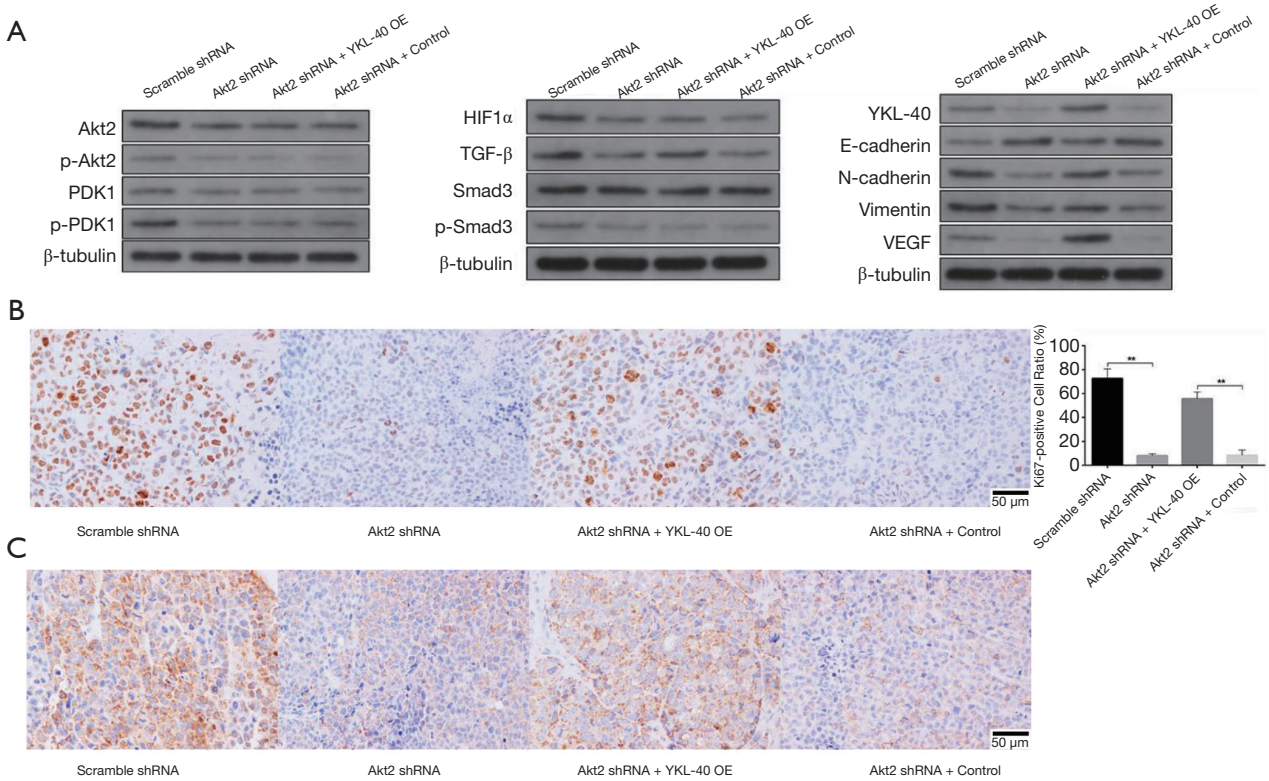

Figure 7 YKL-40-induced angiogenesis and tumor proliferation *in vivo*. (A) WB band map of several total protein factors in different groups of mice tumor cells. (B) Representative Ki67 immunostained tumor tissue slice; Ki67 positive cell ratio of tumor cells. (C) Representative vWF immunostained tumor tissue slice. Scale bars =50 μm (B,C). **, P<0.01.

progression of malignant tumors and angiogenesis. A hypoxic tumor microenvironment induces the accumulation of Akt and Akt phosphorylation in mitochondria of tumor cells. Subsequently, p-Akt promotes PDK1 phosphorylating in mitochondria. The increased level of p-PDK1 upregulates the level of HIF1α by inhibiting the degradation of HIF1α through PHD-pVHL. HIF1α promotes TGFβ/Smad3 signaling through phosphorylation of Smad3, and the latter induces YKL-40 expression. Levels of VEGF, N-cadherin, and Vimentin are boosted by YKL-40. Changes in these factors appear to improve the tumor cells' abilities of proliferation, migration, and invasion and increase tumor neovascularization (*Figure 8*).

Our study is a supplement of the cognizance about the method of tumor resisting hypoxia and the association between hypoxia and YKL-40, to which increasing attention has been paid, and VEGF, which has received recent therapeutic success in lung cancer treatment in relation to the Akt-PDK1 signaling pathway. It may provide new targets for drug discoveries targeted at impeding tumor progression.

Akt is a critical molecule which coordinates complex intracellular signaling pathways and was explored in relation to its association with mitochondria in cellular apoptosis and metabolization (31-34). After Akt was found in mitochondria in its phosphorylated, active state, following stimulation, modulating metabolic related enzymes for the first time (35), the mitochondrial Akt was richly explored for its bioenergetics and tumor cellular survival-regulating function (9,35-38). Our study supplement understanding of of the Akt function in mitochondria. Furthermore, in our study, only two Western blot assays of Akt and PDK1 set COX4 as an internal reference of mitochondrial proteins, and all other assays set β-tubulin for cytoplasm proteins when Akt and PDK1 were included. The changes and quantity rate of (p-)Akt/(p-)PDK1 showed a similar band map in total and mitochondrial protein tests, which may suggest the uniformity in the functions of Akt in relation to mitochondria and more broadly.

Our study had several limitations. We tested the cellular proteins using Western blot assay, which was a

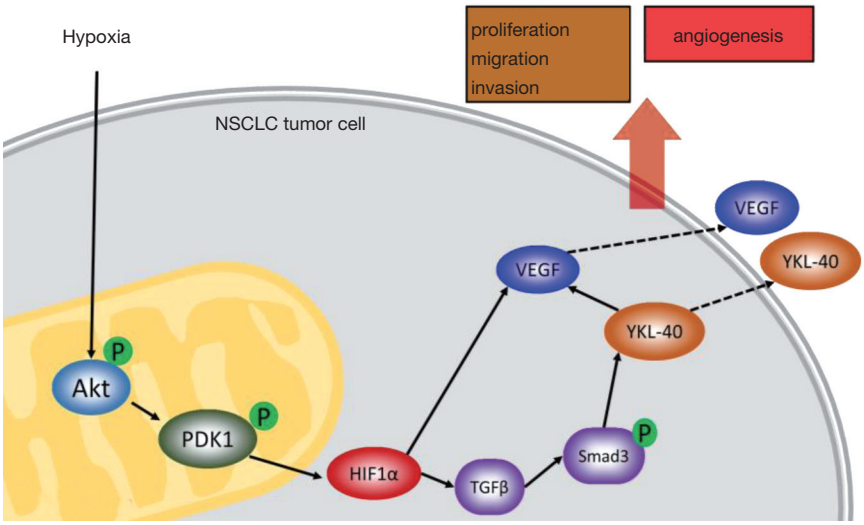

Figure 8 Model illustrating hypoxia-induced tumor malignancy and angiogenesis that is mediated by Akt-PDK1-HIF1α pathway.

semiquantitative protein measurement tool. This may have resulted in some slight or moderate changes being overlooked, and so further research is suggested to achieve more precise measurements and experimental design.

Further exploration of the Akt-PDK1-HIF1α-YKL-40 pathway is needed before a new method of regulation can be recommended, and more accurate regulation details relating to gene edition, transcription, and protein modification are required.

Acknowledgments

Funding: General Program of National Nature Science Foundation of China (Grant No. 81670015 and Grant No. 81370137), Shanghai Pujiang Program (16PJD006).

Footnote

Conflicts of Interest: All authors have completed the ICMJE uniform disclosure form (available at http://dx.doi.org/10.21037/tcr.2020.03.80). The authors have no conflicts of interest to declare.

Ethical Statement: The authors are accountable for all aspects of the work in ensuring that questions related to the accuracy or integrity of any part of the work are appropriately investigated and resolved. Our study was approved by the Animal Ethics Committee of the Second Military Medical University (No. 2018710363).

References

1. Weber M, McWilliams A, Canfell K. Prospects for cost-effective lung cancer screening using risk calculators. Transl Cancer Res 2019;8:S141-4.
2. Hockel M, Vaupel P. Tumor hypoxia: definitions and current clinical, biologic, and molecular aspects. J Natl Cancer Inst 2001;93:266-76.
3. Carmeliet P, Jain RK. Angiogenesis in cancer and other diseases. Nature 2000;407:249-57.
4. Sofia K, Serafim K, Paleolog EM. Hypoxia--a key regulator of angiogenesis and inflammation in rheumatoid arthritis. Nat Rev Rheumatol 2012;8:153.
5. Ma R, He X, Wang H, et al. Hypoxic microenvironment promotes proliferation and invasion of non-small cell lung cancer A549 cells through Wnt/β-catenin signaling pathway. Biomed Res 2018;29:268-73.
6. Yang Y, Wu B, Huang L, et al. Biosimilar candidate IBI305 plus paclitaxel/carboplatin for the treatment of non-

squamous non-small cell lung cancer. Transl Lung Cancer Res 2019;8:989-99.
7. Soni S, Padwad YS. HIF-1 in cancer therapy: two decade long story of a transcription factor. Acta Oncol 2017;56:503-15.
8. Cheng X, Qiu J, Wang S, et al. Comprehensive circular RNA profiling identifies CircFAM120A as a new biomarker of hypoxic lung adenocarcinoma. Ann Transl Med 2019;7:442.
9. Chae YC, Vaira V, Caino MC, et al. Mitochondrial Akt Regulation of Hypoxic Tumor Reprogramming. Cancer Cell 2016;30:257-72.
10. Sutendra G, Dromparis P, Kinnaird A, et al. Mitochondrial activation by inhibition of PDKII suppresses HIF1a signaling and angiogenesis in cancer. Oncogene 2013;32:1638-50.
11. Maynard MA, Ohh M. The role of hypoxia-inducible factors in cancer. Cell Mol Life Sci 2007;64:2170-80.
12. Jaakkola P, Mole DR, Tian YM, et al. Targeting of HIF-alpha to the von Hippel-Lindau ubiquitylation complex by O2-regulated prolyl hydroxylation. Science 2001;292:468-72.
13. Sun W, Zhou S, Chang SS, et al. Mitochondrial mutations contribute to HIF1alpha accumulation via increased reactive oxygen species and up-regulated pyruvate dehydrogenease kinase 2 in head and neck squamous cell carcinoma. Clin Cancer Res 2009;15:476-84.
14. Lu H, Dalgard CL, Mohyeldin A, et al. Reversible inactivation of HIF-1 prolyl hydroxylases allows cell metabolism to control basal HIF-1. J Biol Chem 2005;280:41928-39.
15. Ke S, Chen S, Dong Z, et al. Erythrocytosis in hepatocellular carcinoma portends poor prognosis by respiratory dysfunction secondary to mitochondrial DNA mutations. Hepatology 2017;65:134-51.
16. Kushida N, Nomura S, Mimura I, et al. Hypoxia-Inducible Factor-1alpha Activates the Transforming Growth Factor-beta/SMAD3 Pathway in Kidney Tubular Epithelial Cells. Am J Nephrol 2016;44:276-85.
17. Suwanabol PA, Seedial SM, Shi X, et al. Transforming growth factor-beta increases vascular smooth muscle cell proliferation through the Smad3 and extracellular signal-regulated kinase mitogen-activated protein kinases pathways. J Vasc Surg 2012;56:446-54.
18. Tsai S, Hollenbeck ST, Ryer EJ, et al. TGF-beta through Smad3 signaling stimulates vascular smooth muscle cell proliferation and neointimal formation. Am J Physiol Heart Circ Physiol 2009;297:H540-9.
19. Shi X, Guo LW, Seedial SM, et al. TGF-beta/Smad3 inhibit vascular smooth muscle cell apoptosis through an autocrine signaling mechanism involving VEGF-A. Cell Death Dis 2014;5:e1317.
20. Qiu QC, Wang L, Jin SS, et al. CHI3L1 promotes tumor progression by activating TGF-beta signaling pathway in hepatocellular carcinoma. Sci Rep 2018;8:15029.
21. Joseph JV, Conroy S, Tomar T, et al. TGF-β is an inducer of ZEB1-dependent mesenchymal transdifferentiation in glioblastoma that is associated with tumor invasion. Cell Death Dis 2014;5:e1443.
22. Jefri M, Huang YN, Huang WC, et al. YKL-40 regulated epithelial-mesenchymal transition and migration/invasion enhancement in non-small cell lung cancer. BMC Cancer 2015;15:590.
23. Kawada M, ., Seno H, ., Kanda K, ., et al. Chitinase 3-like 1 promotes macrophage recruitment and angiogenesis in colorectal cancer. Oncogene 2012;31:3111-23.
24. Francescone RA, Scully S, Faibish M, et al. Role of YKL-40 in the angiogenesis, radioresistance, and progression of glioblastoma. J Biol Chem 2011;286:15332-43.
25. Shao R. YKL-40 acts as an angiogenic factor to promote tumor angiogenesis. Front Physiol 2013;4:122.
26. Francescone R, Ngernyuang N, Yan W, et al. Tumor-derived mural-like cells coordinate with endothelial cells: role of YKL-40 in mural cell-mediated angiogenesis. Oncogene 2014;33:2110-22.
27. Kzhyshkowska J, Yin S, Liu T, et al. Role of chitinase-like proteins in cancer. Biol Chem 2016;397:231-47.
28. Libreros S, Iragavarapu-Charyulu V. YKL-40/CHI3L1 drives inflammation on the road of tumor progression. J Leukoc Biol 2015;98:931-6.
29. Riabov V, Gudima A, Wang N, et al. Role of tumor associated macrophages in tumor angiogenesis and lymphangiogenesis. Front Physiol 2014;5:75.
30. Serrano-Gomez SJ, Maziveyi M, Alahari SK. Regulation of epithelial-mesenchymal transition through epigenetic and post-translational modifications. Mol Cancer 2016;15:18.
31. Parcellier A, Tintignac LA, Zhuravleva E, et al. PKB and the mitochondria: AKTing on apoptosis. Cell Signal 2008;20:21-30.
32. Zhou H, Li XM, Meinkoth J, et al. Akt regulates cell survival and apoptosis at a postmitochondrial level. J Cell Biol 2000;151:483-94.
33. Stiles BL. PI-3-K and AKT: Onto the mitochondria. Adv Drug Deliv Rev 2009;61:1276-82.
34. Hers I, Vincent EE, Tavaré JM. Akt signalling in health and disease. Cell Signal 2011;23:1515-27.

35. Bijur GN, Jope RS. Rapid accumulation of Akt in mitochondria following phosphatidylinositol 3-kinase activation. J Neurochem 2003;87:1427-35.
36. Mcbride HM, Neuspiel M, Wasiak S. Mitochondria: More Than Just a Powerhouse. Curr Biol 2006;16:R551-60.
37. Ghosh JC, Siegelin MD, Valentina V, et al. Adaptive mitochondrial reprogramming and resistance to PI3K therapy. J Natl Cancer Inst 2015;107. doi: 10.1093/jnci/dju502.
38. Bijur GN, Jope RS. Glycogen synthase kinase-3 beta is highly activated in nuclei and mitochondria. Neuroreport 2003;14:2415-9.

Cite this article as: Miao Y, Wang W, Dong Y, Hu J, Wei K, Yang S, Lai X, Tang H. Hypoxia induces tumor cell growth and angiogenesis in non-small cell lung carcinoma via the Akt-PDK1-HIF1α-YKL-40 pathway. Transl Cancer Res 2020;9(4):2904-2918. doi: 10.21037/tcr.2020.03.80

Supplementary

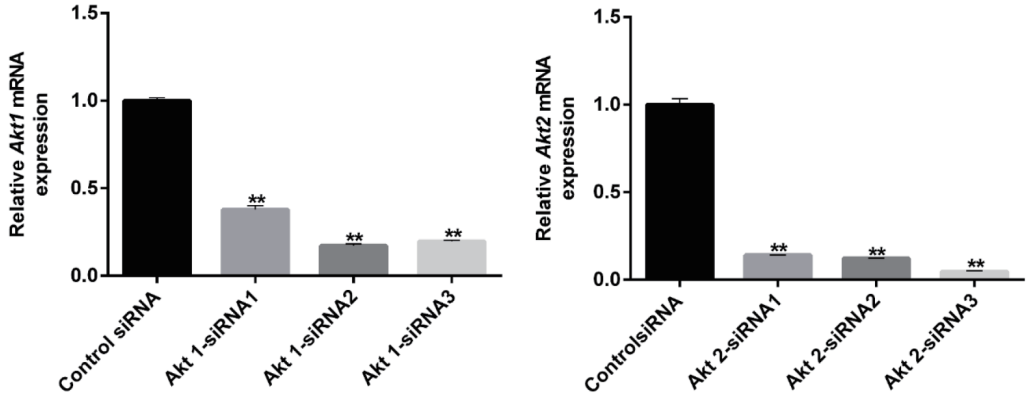

Figure S1 Relative Akt1/Akt2 mRNA expression in CL1-5 cells that were interfered by 3 different artificial siRNAs or the control siRNA (control siRNA =1.0); employing qRT-PCR to verify the effects. Akt1-siRNA2 and Akt2-siRNA3 were chosen as Akt1-siRNA and Akt2-siRNA to participate in the following experiments. **, P<0.01 *vs.* NC.

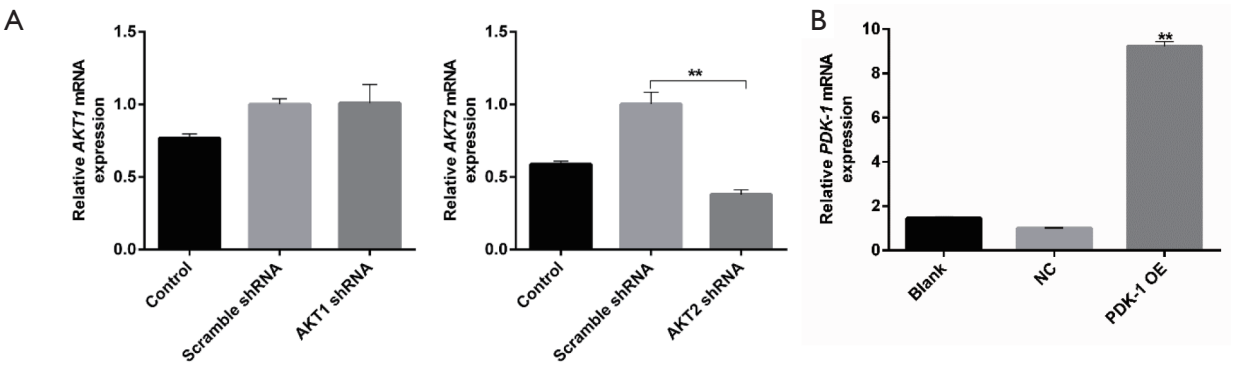

Figure S2 Akt2 shRNA and PDK1 OE mRNA expression verified by qRT-PCR. (A) Relative Akt1/Akt2 mRNA expression in Akt1/Akt2 shRNA lentiviral vector stably transfected CL1-5 cells; control, without any treatment; scramble shRNA, transfected by scramble shRNA interfering plasmid; Akt1/Akt2 shRNA, transfected by Akt1/Akt2 shRNA interfering plasmid (scramble shRNA =1.0) Akt2 shRNA stably transfected CL1-5 cell was effective (P<0.01) (B) Relative PDK1 mRNA expression in CL1-5 cells. It was confirmed that PDK1 OE transfection succeeded; blank, without any treatment; NC, negative control, transfected by blank vector; PDK1 OE, transfected by PDK1 overexpression vector. **, P<0.01 *vs.* NC.

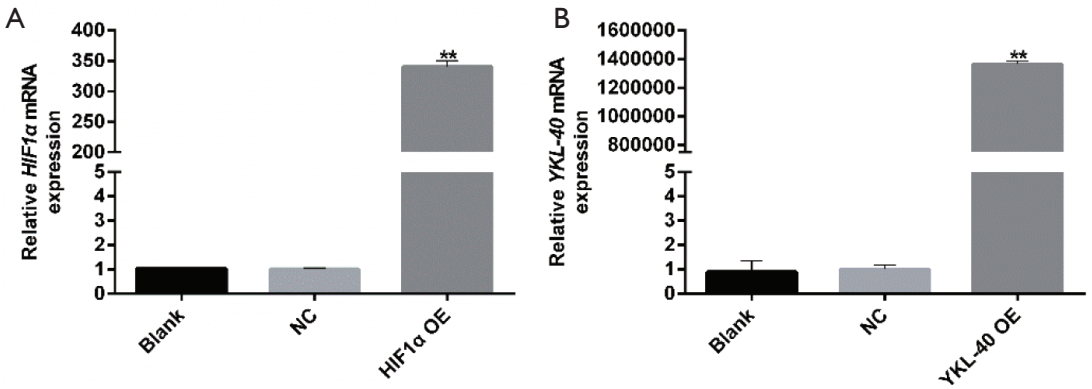

Figure S3 HIF1α and YKL-40 OE mRNA expression verified by qRT-PCR. (A) Relative HIF1α mRNA expression in CL1-5 cells; blank, without any treatment; NC, negative control, transfected by blank vector; HIF1α OE, transfected by HIF1α overexpression vector. (B) Relative YKL-40 mRNA expression in CL1-5 cells confirmed by qRT-PCR; YKL-40 OE, transfected by YKL-40 overexpression vector. **, P<0.01 *vs*. NC.